NANO LETTERS

Letter

pubs.acs.org/NanoLett

The Nature of the Interlayer Interaction in Bulk and Few-Layer Phosphorus

L. Shulenburger,[†] A.D. Baczewski,[†] Z. Zhu,[‡] J. Guan,[‡] and D. Tománek*[,‡]

[†]Sandia National Laboratories, Albuquerque, New Mexico 87185, United States

[‡]Physics and Astronomy Department, Michigan State University, East Lansing, Michigan 48824, United States

Supporting Information

ABSTRACT: Sensitive dependence of the electronic structure on the number of layers in few-layer phosphorene raises a question about the true nature of the interlayer interaction in so-called "van der Waals (vdW) solids". We performed quantum Monte Carlo calculations and found that the interlayer interaction in bulk black phosphorus and related few-layer phosphorene is associated with a significant charge redistribution that is incompatible with purely dispersive forces and not captured by density functional theory calculations with different vdW corrected functionals. These findings confirm the necessity of more sophisticated treatment of nonlocal electron correlation in total energy calculations.

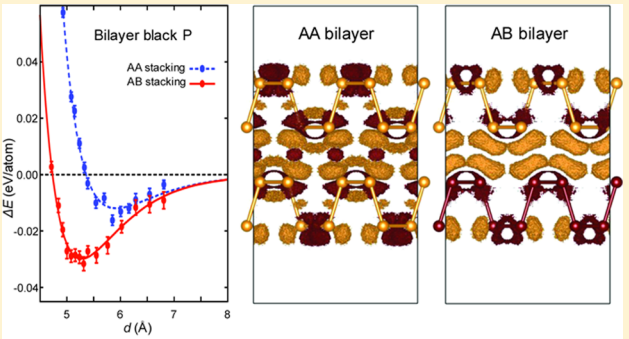

Interaction energy and charge redistribution in a bilayer of black phosphorus

KEYWORDS: *Phosphorus, phosphorene, ab initio, interlayer interaction*

There is growing interest in understanding and correctly describing the nature of the weak interlayer interaction in layered systems ranging from few-layer graphene[1] to transition metal dichalcogenides[2] such as MoS_2 and few-layer phosphorene,[3,4] which display unique electronic properties and bear promise for device applications. Anticipating that challenges concerning the stability and isolation of single- to few-layer phosphorene can be overcome,[5] this system with its unique electronic[3,4] and optical[6] properties is attracting particular interest. It displays a high and anisotropic carrier mobility[7,8] and a robust band gap that depends sensitively on the in-layer strain.[3] Progress in device fabrication[4,9] indicates clearly that phosphorene holds technological promise. Because the fundamental band gap depends sensitively on the number of layers,[3] understanding the nature of the interlayer interaction is particulary important.

The standard approach to describe the interlayer interaction in layered solids has been based on density functional theory (DFT). Whereas in principle, DFT is capable of describing the total energy of any system in the ground state exactly, current implementations describe the effects of electron exchange and correlation only in an approximate manner. In most covalent and ionic solids of interest, the specific treatment of exchange and correlation of electrons does not play a crucial role and commonly used local or semilocal exchange-correlation functionals of the electron density are adequate. This approach may, however, not be adequate in complex and weakly bonded systems[10] including black phosphorus.[11] This is illustrated in Figure 1, which displays large differences between interlayer interaction energies in bulk and bilayer black phosphorus, obtained using different DFT functionals contained in the VASP software package.[12−14] The large spread of the interlayer energies predicted using these functionals, some of which include van der Waals (vdW) corrections, illustrates the gravity of the issue.

Even though vdW corrected exchange-correlation functionals can improve the predicted geometry of layered phosphorus, other quantities such as the transition pressure from bulk orthorhombic to rhombohedral phases are significantly underestimated.[11] This comes as no surprise, because recent benchmarks in graphene indicate that significant variations in the relative accuracy are observed among numerous vdW corrected functionals.[25]

A superior way to obtain insight into the nature of the interlayer interaction requires a computational approach that treats electron exchange and correlation adequately and on the same footing as covalent and ionic interactions. Distinct from DFT, the fundamental quantity in quantum Monte Carlo (QMC) calculations is the properly antisymmetrized all-valence-electron wave function that explicitly describes the correlation of electrons. Therefore, the weak interlayer interaction in layered systems obtained using QMC is expected to be more precise than the DFT-based counterpart, and the electron density obtained by QMC likely provides a better representation of the true charge density than DFT. Should the QMC-based electron distribution in a few-layer system differ in

Received: September 8, 2015
Revised: October 28, 2015
Published: November 2, 2015

DOI: 10.1021/acs.nanolett.5b03615
Nano Lett. 2015, 15, 8170−8175

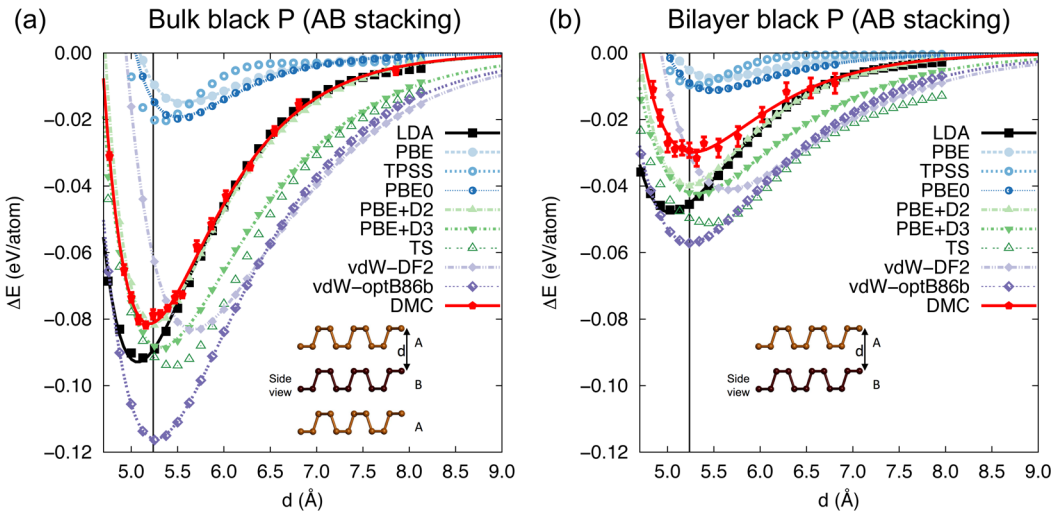

Figure 1. Binding energy per atom ΔE as a function of the interlayer spacing d in AB stacked (a) bulk and (b) bilayer black phosphorus. QMC results obtained using DMC are compared to DFT with LDA,[15] PBE,[16] TPSS,[17] PBE0,[18] PBE+D2,[19] PBE+D3,[20] TS,[21] vdW-DF2,[22] and vdW-optB86b[23,24] exchange-correlation functionals. The lines connecting the data points are Morse fits that extrapolate to $\Delta E = 0$ for $d \rightarrow \infty$. The vertical dashed line indicates the observed interlayer spacing d_e(expt.) = 5.2365 Å in the bulk structure in (a) and the optimum value based on DMC in the bilayer in (b). Side views of the geometries are shown in the insets.

a significant and nontrivial manner from a superposition of electron densities in isolated monolayers, we may surely conclude that the interlayer interaction in such a system is not of a simple additive dispersive nature.

In the past decade, QMC methods have demonstrated considerable promise as a high-accuracy first-principles method for studying solids[26] and are especially well-suited to so-called "vdW solids".[27−33] On one hand, the absence of approximations in treating the interaction between electrons makes it an ideal method for layered materials with a competition between different types of interactions. On the other hand, the computational cost associated with QMC calculations is typically 1000−10 000 times higher than that of comparable semilocal DFT calculations. Even though this cost is mitigated by its superior parallel scalability, for the time being QMC is most useful for benchmark calculations.

We have performed QMC calculations for bulk and bilayer black phosphorus using the approach described in the Methods section. Our diffusion Monte Carlo (DMC) results for the interlayer binding curves in these systems are shown by the solid lines in Figure 1. The total energy difference between the monolayer and the bulk system indicates that the binding energy of phosphorene sheets in black phosphorus is 81 ± 6 meV/atom, which translates to a cleavage energy of 22.4 ± 1.6 meV per Å^2 of the interface area although this value may be slightly reduced by vibrational free energy. This is larger than that for many other layered materials[34] but weak enough to allow mechanical exfoliation that has been reported.[3,4]

Comparing the DMC results to a variety of different DFT functionals, significant variability is evident. Results for LDA, PBE, TPSS and PBE0, which do not treat vdW explicitly, are in agreement with intuition, namely, that LDA overbinds and reduces the interlayer spacing in comparison to experiment whereas PBE, TPSS, and PBE0 underbind. This sequence of functionals also illustrates the effect of varying treatments of exchange and static semilocal correlation corresponding to various rungs of "Jacob's Ladder".[35]

From the wide array of available vdW functionals, we have selected several that are exemplary of different philosophies of construction. PBE+D2 is based upon an empirical correction to the total energy in the form of a simple pairwise interaction parametrized by atomic C_6 coefficients. The D3 and TS approaches refine this basic approach with an increased dependence on environment. vdW-optB86b and vdW-DF2 represent a different approach based solely on the global charge density and ignoring ionic coordinates; these functionals are both based upon improvements to the nonlocal vdW-DF functional.[36] Significant variability is evident in both energetics and the equilibrium interlayer spacing among these functionals. It is interesting to note that the least sophisticated of these functionals (PBE+D2) performs the best relative to both DMC and the experiment in the case of the bulk system. However, there is reason to believe that the agreement of this pairwise additive functional with DMC is fortuitous as will be shortly described.

Contrasting the bulk and bilayer binding curves, it is evident that DMC predicts that the interlayer interaction is not strictly additive. For an additive interaction, we should expect that the binding energy of the bilayer would be approximately one-half that of the bulk system, because both layers are missing half of their neighboring layers. DMC predicts that this is not the case and that the bilayer binding energy is three-eighths that of the bulk system instead. The results for vdW corrected DFT (PBE+D2, PBE+D3, TS, vdW-optB86b, and vdW-DF2) are more indicative of an additive interlayer interaction, giving us another indication that the nature of the interlayer binding in black phosphorus is richer than a simple vdW interaction.

A more direct indication of the character of the interlayer binding is the charge density difference induced by assembling the bulk system from isolated monolayers. We computed the quantity $\Delta\rho = \rho_{tot}(\text{bulk}) - \sum\rho_{tot}(\text{monolayers})$ using both DMC and DFT to investigate this. The l_1-norm of $\Delta\rho$ over the unit cell[37] is an indicator of the number of electrons being redistributed due to interlayer interaction. This metric indicates a motion of fewer than 0.03 electrons per atom in all DFT functionals considered in this study. In contrast, DMC predicts a more significant redistribution of 0.15 electrons per atom. To provide insight into the nature of this charge redistribution, the

DOI: 10.1021/acs.nanolett.5b03615
Nano Lett. 2015, 15, 8170−8175

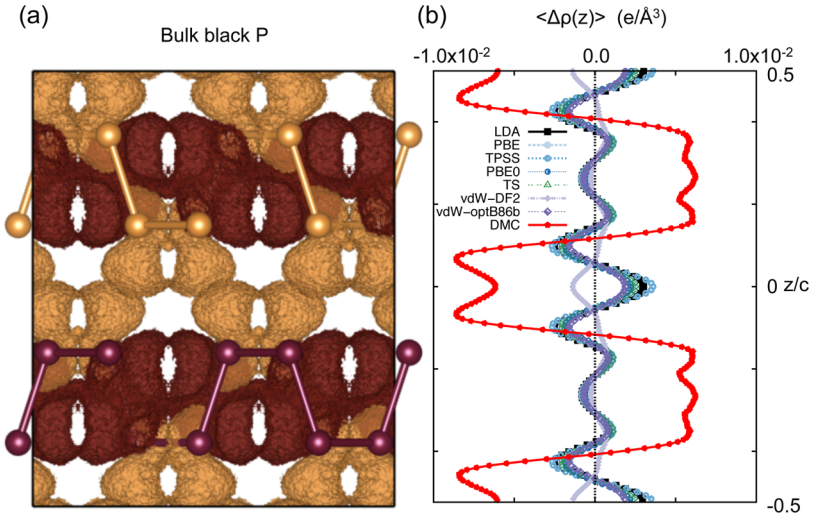

Figure 2. Electron density difference $\Delta\rho = \rho_{tot}(\text{bulk}) - \sum \rho_{tot}(\text{monolayers})$ representing the charge redistribution caused by assembling the bulk structure from isolated monolayers. (a) DMC isosurfaces bounding regions of excess electron density (dark brown) and electron deficiency (light brown) with respective values $\pm 6.5 \times 10^{-3}$ e/Å^3. (b) $\langle \Delta\rho(z) \rangle$ for DMC and several DFT functionals averaged across the x−y plane of the layers with z/c indicating the relative position of the plane in the unit cell. Note that TS and PBE give the same charge densities by construction, as would PBE+D2 and PBE+D3 (not shown).

corresponding density difference is visualized in Figure 2a. Inspection indicates that charge is pushed out of the region between layers and into the covalent bonds within each layer. This picture is well supported by basic chemical intuition. In an isolated layer, each atom is 3-fold coordinated with sp^3 bonding character and a single lone pair protruding away from the layer. Bringing layers together will increase the overlap between these lone pairs on adjacent layers and steric forces will tend to drive the affiliated lone pair charge closer to the layer, on which it originated.

To further elucidate the role that this charge redistribution plays in the interlayer binding, the planar average of the charge density difference along planes perpendicular to the interlayer axis for both DMC and several DFT functionals are illustrated in Figure 2b. It remains evident that DMC predicts an average depletion of charge between the layers with two depletion maxima and commensurate accumulation within the layers. However, with the exception of vdW-DF2 this trend is not evident in any of the DFT calculations. Instead, DFT predicts a weak accumulation of charge between layers with a simpler structure. The case of vdW-DF2 is of particular interest, because it is the only functional that predicts a qualitatively similar but considerably weaker trend as DMC. Even so, the fact that PBE+D2 performs best in terms of energetics and geometry indicates that this functional may be getting the right answer for reasons that are not necessarily consistent with the many-body physics more explicitly explored through DMC. This situation is especially troubling as the charge density is the central quantity in DFT and indications that this quantity is not accurately reproduced for black phosphorus cast into doubt other properties derived from such DFT calculations. Additionally, changing the treatment of exchange (illustrated by the sequence LDA, PBE, TPSS, PBE0) does not significantly affect the charge redistribution, likely pointing to electron correlation as the problematic part of the interlayer interaction.

Recent work on self-consistent vdW functionals indicates that the charge redistribution induced by vdW interactions can play an important role in the energetics of highly polarizable systems.[38] In this work, the authors note that this subtle physics is consistent with an early observation by Feynman[39] in which the vdW interaction can be viewed as arising from an attractive interaction induced through a small accumulation of charge density between two mutually perturbed neutral systems. In the case of black phosphorus, we find that this picture of the vdW interaction is balanced by the steric redistribution of charge away from the region between layers. Upon the basis of the results elucidated by our DMC calculations, we anticipate that getting this balance right may be a critical requirement to examine in developing more advanced DFT functionals for layered compounds. Indeed, the fact that current DFT functionals predict charge redistribution greatly at odds with DMC shows that merely the inclusion of steric effects is insufficient to capture the nature of bonding in this system.

The corresponding difference between the charge density in an isolated monolayer and in a layer within bulk phosphorus is likely to affect the in-plane bonding and geometry. To see if this is indeed the case, we have calculated the energy change ΔE as a function of a stretch applied along the softer axis $\vec{a}_1$ of the sheets. Our results for the bulk system, presented in Figure 3, indicate an excellent agreement (to within half a percent) between the optimized lattice constant $a_1(\text{theory}) = 4.404 \pm 0.019$ Å and the observed value[40] $a_1(\text{expt.}) = 4.374$ Å in the bulk structure. Further, we can see precisely how soft this axis is in both systems with a deformation by $|\Delta a_1| \lesssim 0.3$ Å requiring an energy investment of only ∼5 meV/atom in a monolayer or in bulk black phosphorus. This energy corresponds to a thermal energy of 60 K, and we should expect significant thermal fluctuations of the geometry of unsupported phosphorene sheets at ambient temperature and pressure. Most important, however, is the comparison between a_1 in the isolated monolayer and in the bulk structure. Our DMC results indicate a change in the in-plane stiffness along the soft axis and an ∼2% reduction in the equilibrium lattice constant a_1 in a monolayer from the bulk value. This is another indication of a charge redistribution during the formation of a layered bulk structure from monolayers that modifies the covalent interaction within the layers. This again supports our finding that the interlayer interaction in black phosphorus is not purely dispersive.

DOI: 10.1021/acs.nanolett.5b03615
Nano Lett. 2015, 15, 8170−8175

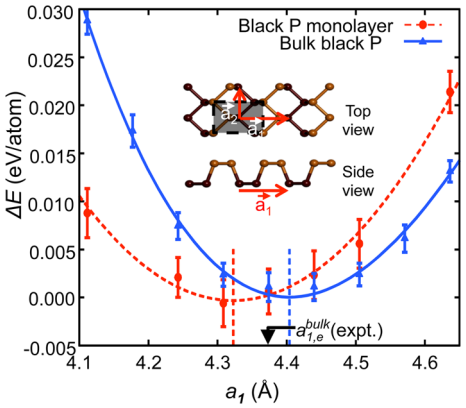

Figure 3. DMC results for the relative total energy per atom ΔE as a function of the in-layer lattice constant a_1 in the soft direction of a phosphorene monolayer and of bulk black phosphorus. The lines connecting the data points are fits with cubic polynomials and the minima of the fits are taken to be $\Delta E = 0$. The optimum lattice constant values for both structures are indicated by the vertical dashed lines. The observed value $a_{1,e}$(expt.) = 4.374 Å in the bulk structure is indicated by the arrow. The monolayer geometry is shown in the inset.

To gain additional insight into the nature of the interlayer interaction, we compare in Figure 4 the bonding within an AA and AB stacked bilayer as a function of the interlayer separation d. Our DMC results in Figure 4 indicate that the AB stacking, which occurs in the bulk material, persists also in the bilayer.

The cleavage energy of an AB stacked bilayer is 16.6 ± 2.2 meV/Å^2, thus 26% smaller than the bulk cleavage energy of 22.4 ± 1.6 meV/Å^2. The exfoliation energy associated with removing the topmost layer from the surface is expected to lie between these two values. These findings appear plausible also because in graphite the cleavage energy is estimated to be 18% larger than the exfoliation energy.[41] Though we expect the interlayer interaction to be mediated primarily by the π-electrons in graphite and sp^3-like lone pairs with a different character in black phosphorus, the ratio of the exfoliation and cleavage energy in the two systems appears to be close.

The interlayer spacing d_e = 5.272 ± 0.023 Å in the AB-stacked bilayer is about 1% larger than our calculated value for the bulk material. In the less favorable AA stacking geometry, the binding energy is three times smaller than in the AB geometry, which should effectively prevent formation of stacking faults at least in the absence of impurities. The significant difference between the interaction in the AA and AB stacked bilayer suggests that the interaction between the sheets is more complicated than the vdW interaction between two homogeneous slabs. Were the interlayer interaction purely dispersive, the registry of layers would not matter much and the AA and AB binding energies as well as interlayer separations should be nearly identical. Indeed, bilayer graphene exhibits a change of only ∼0.1 Å in interlayer spacing and ∼55% (∼6 meV per atom) in binding energy when changing from an AA to an AB geometry[25] in contrast to the ∼0.6 Å and ∼150% (∼18 meV) difference in phosphorene.

To shed some light on the sensitivity of the interlayer bonding on the stacking sequence, we investigated the change in the charge density $\Delta\rho$ induced by the interaction. Our results for AB and AA stacking are shown in Figure 4c. Similar to the corresponding results for bulk black phosphorus in Figure 2b, the $\Delta\rho$ plots for the bilayer show a significant rearrangement of the electronic charge, that is, a total of ∼0.075 electrons per atom in both cases. In the AB-stacked bilayer, similar to the bulk system, we observe a depletion of the electron density in the region between the sheets and electron accumulation within the layers. The charge redistribution in the AA bilayer is significantly different, even including small regions in the interlayer space where the charge density increases. The large difference between $\Delta\rho$ in the AA and AB stacked bilayer is

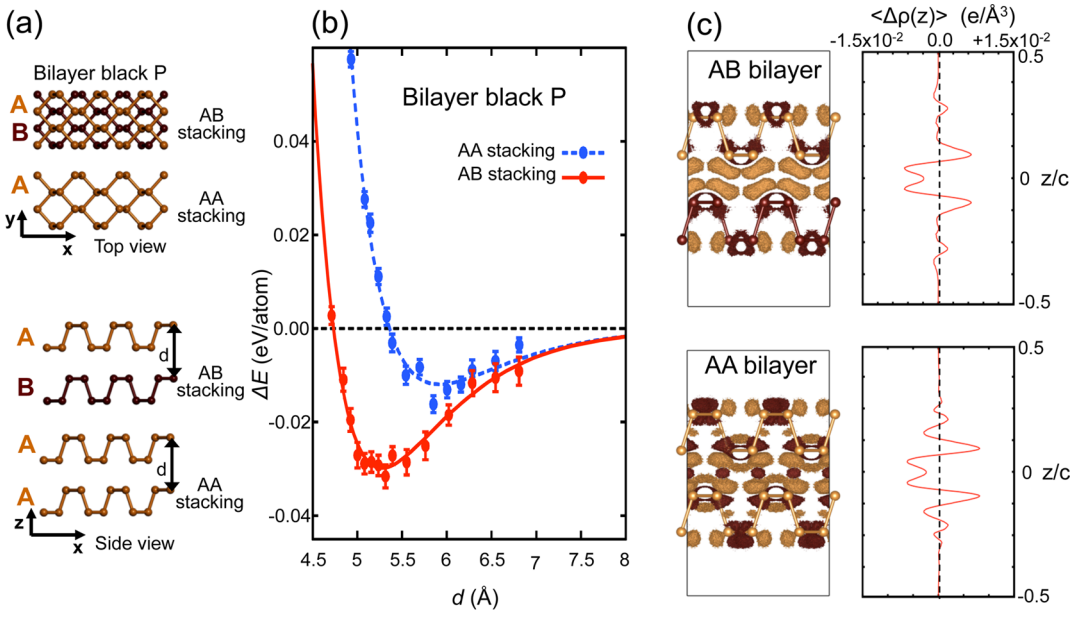

Figure 4. DMC results for bonding in AA and AB stacked phosphorene bilayers. (a) Geometry of an AA and AB stacked bilayer in top and side view. (b) DMC results for the relative total energy per atom ΔE as a function of the interlayer spacing d. The lines connecting the data points are Morse fits that extrapolate to $\Delta E = 0$ for $d \to \infty$. (c) Electron density differences for the AB and AA bilayers illustrated using isosurfaces and planar averaging as in Figure 2 (with the same color coding). Note that the planar averaging over all space results in a net depletion of charge between the layers even for the AA stacked case.

DOI: 10.1021/acs.nanolett.5b03615
Nano Lett. 2015, 15, 8170−8175

inconsistent with purely dispersive bonding and explains why the interlayer spacing and binding energy are so different in the two systems. We have applied the same methodology to AA and AB stacked graphene as in ref 25. Consistent with the interpretation of graphene as a van der Waals system, we find charge redistribution virtually identical to that predicted by DFT.

In summary, we studied the nature of the interlayer interaction in layered black phosphorus using quantum Monte Carlo calculations, which describe the correlation of electrons explicitly by an antisymmetrized all-valence-electron Green's function and treat covalent and dispersive interactions on the same footing. The approach is similar but more flexible than wave function-based approaches such as the random phase approximation that might provide a compromise between the accuracy of DMC and the efficiency of DFT.[42] Unlike in true vdW systems, we find that the interlayer interaction in few-layer phosphorene is associated with a significant charge redistribution between the in-layer and interlayer region, caused by changes in the nonlocal correlation of electrons in adjacent layers. Consequently, the resulting interlayer interaction can not be described properly by DFT augmented by mere semilocal vdW correction terms, and thus the designation "van der Waals solids" is strictly improper for systems including few-layer phosphorene. We also tested several nonlocal DFT functionals designed to capture van der Waals effects and have found that the tested formulations do not quantitatively reproduce the charge reorganization found using DMC. Our results may be used as benchmarks for developing more sophisticated DFT functionals that should provide an improved description of nonlocal electron correlation in layered systems. In particular, we note that one nonlocal vdW functional, vdW-DF2, was able to qualitatively but not quantitatively capture the charge redistribution, suggesting an important avenue for further functional development.

Methods. Our QMC calculations are based on the diffusion Monte Carlo (DMC) approach used in QMCPACK[43,44] with an exhaustive description of the methodological details given in ref 26. This computational technique, along with details of the pseudopotential and an intensive procedure for converging finite-size effects, is described in the Supporting Information. One of the key limitations in our calculation is the bias due to a fixed nodal surface. This was not anticipated to be significant in black phosphorus as the binding of interest occurs in a region of low electronic density for which the degree of nodal nonlinearity is expected to be low.[45] Nevertheless, some DMC calculations were carried out using orbitals from LDA, PBE, and vdW-optb86B functionals to investigate the impact of the fixed node approximation. As the nodal surface associated with LDA orbitals were found to give the lowest energy and our method is variational, the LDA orbitals were subsequently used in all cases.

■ ASSOCIATED CONTENT

Supporting Information

The Supporting Information is available free of charge on the ACS Publications website at DOI: 10.1021/acs.nanolett.5b03615.

Methodological details of our QMC and comparative DFT calculations, along with details of the pseudopotential and an intensive procedure for converging finite-size effects, as well as results for different stacking geometries. (PDF)

■ AUTHOR INFORMATION

Corresponding Author

*E-mail: tomanek@pa.msu.edu.

Notes

The authors declare no competing financial interest.

■ ACKNOWLEDGMENTS

We are grateful for useful comments and conversations with Paul Kent, Jeongnim Kim, Ann Mattsson, Jonathan Moussa, Lydia Nemec, and Gotthard Seifert. Calculations were performed on *Sequoia* at Lawrence Livermore National Laboratory and *Mira* at the Argonne Leadership Computing Facility. We thank Anouar Benali for assistance performing calculations on *Mira*. An award of computer time was provided by the Innovative and Novel Computational Impact on Theory and Experiment (INCITE) program with Project CPH103. A.B. and L.S. were supported through the Predictive Theory and Modeling for Materials and Chemical Science program by the Office of Basic Energy Sciences (BES), Department of Energy (DOE). Z.Z., J.G., and D.T. acknowledge partial support by the National Science Foundation Cooperative Agreement No. EEC-0832785, titled "NSEC: Center for High-Rate Nanomanufacturing". J.G. and D.T. also acknowledge partial support by the NSF/AFOSR EFRI 2-DARE Grant EFMA-1433459. Sandia National Laboratories is a multiprogram laboratory managed and operated by Sandia Corporation, a wholly owned subsidiary of Lockheed Martin Corporation, for the U.S. Department of Energy's National Nuclear Security Administration under contract DE-AC04-94AL85000.

■ REFERENCES

(1) Novoselov, K. S.; Jiang, D.; Schedin, F.; Booth, T. J.; Khotkevich, V. V.; Morozov, S.; Geim, A. *Proc. Natl. Acad. Sci. U. S. A.* **2005**, *102*, 10451−10453.
(2) Zhuang, H. L.; Hennig, R. G. *J. Phys. Chem. C* **2013**, *117*, 20440−20445.
(3) Liu, H.; Neal, A. T.; Zhu, Z.; Luo, Z.; Xu, X.; Tománek, D.; Ye, P. D. *ACS Nano* **2014**, *8*, 4033−4041.
(4) Li, L.; Yu, Y.; Ye, G. J.; Ge, Q.; Ou, X.; Wu, H.; Feng, D.; Chen, X. H.; Zhang, Y. *Nat. Nanotechnol.* **2014**, *9*, 372−377.
(5) Castellanos-Gomez, A.; Vicarelli, L.; Prada, E.; Island, J. O.; Narasimha-Acharya, K. L.; Blanter, S. I.; Groenendijk, D. J.; Buscema, M.; Steele, G. A.; Alvarez, J. V.; Zandbergen, H. W.; Palacios, J. J.; van der Zant, H. S. J. *2D Mater.* **2014**, *1*, 025001.
(6) Tran, V.; Soklaski, R.; Liang, Y.; Yang, L. *Phys. Rev. B: Condens. Matter Mater. Phys.* **2014**, *89*, 235319.
(7) Gillgren, N.; Wickramaratne, D.; Shi, Y.; Espiritu, T.; Yang, J.; Hu, J.; Wei, J.; Liu, X.; Mao, Z.; Watanabe, K.; Taniguchi, T.; Bockrath, M.; Barlas, Y.; Lake, R. K.; Lau, C. N. *2D Mater.* **2015**, *2*, 011001.
(8) Fei, R.; Yang, L. *Nano Lett.* **2014**, *14*, 2884−2889.
(9) Koenig, S. P.; Doganov, R. A.; Schmidt, H.; Castro Neto, A. H.; Özyilmaz, B. *Appl. Phys. Lett.* **2014**, *104*, 103106.
(10) Cicero, G.; Grossman, J. C.; Schwegler, E.; Gygi, F.; Galli, G. *J. Am. Chem. Soc.* **2008**, *130*, 1871−1878.
(11) Appalakondaiah, S.; Vaitheeswaran, G.; Lebègue, S.; Christensen, N. E.; Svane, A. *Phys. Rev. B: Condens. Matter Mater. Phys.* **2012**, *86*, 035105.
(12) Kresse, G.; Furthmüller, J. *Phys. Rev. B: Condens. Matter Mater. Phys.* **1996**, *54*, 11169−11186.
(13) Kresse, G.; Furthmüller, J. *Comput. Mater. Sci.* **1996**, *6*, 15−50.

DOI: 10.1021/acs.nanolett.5b03615
Nano Lett. 2015, 15, 8170−8175

(14) Kresse, G.; Joubert, D. *Phys. Rev. B: Condens. Matter Mater. Phys.* **1999**, *59*, 1758−1775.
(15) Perdew, J. P.; Zunger, A. *Phys. Rev. B: Condens. Matter Mater. Phys.* **1981**, *23*, 5048−5079.
(16) Perdew, J. P.; Burke, K.; Ernzerhof, M. *Phys. Rev. Lett.* **1996**, *77*, 3865−3868.
(17) Tao, J.; Perdew, J. P.; Staroverov, V. N.; Scuseria, G. E. *Phys. Rev. Lett.* **2003**, *91*, 146401.
(18) Adamo, C.; Barone, V. *J. Chem. Phys.* **1999**, *110*, 6158−6170.
(19) Grimme, S. *J. Comput. Chem.* **2006**, *27*, 1787−1799.
(20) Grimme, S.; Antony, J.; Ehrlich, S.; Krieg, H. *J. Chem. Phys.* **2010**, *132*, 154104.
(21) Tkatchenko, A.; Scheffler, M. *Phys. Rev. Lett.* **2009**, *102*, 073005.
(22) Lee, K.; Murray, E. D.; Kong, L.; Lundqvist, B. I.; Langreth, D. C. *Phys. Rev. B: Condens. Matter Mater. Phys.* **2010**, *82*, 081101.
(23) Klimeš, J.; Bowler, D. R.; Michaelides, A. *J. Phys.: Condens. Matter* **2010**, *22*, 022201.
(24) Klimeš, J.; Bowler, D. R.; Michaelides, A. *Phys. Rev. B: Condens. Matter Mater. Phys.* **2011**, *83*, 195131.
(25) Mostaani, E.; Drummond, N. D.; Fal'ko, V. I. *Phys. Rev. Lett.* **2015**, *115*, 115501.
(26) Shulenburger, L.; Mattsson, T. R. *Phys. Rev. B: Condens. Matter Mater. Phys.* **2013**, *88*, 245117.
(27) Drummond, N. D.; Needs, R. J. *Phys. Rev. B: Condens. Matter Mater. Phys.* **2006**, *73*, 024107.
(28) Sorella, S.; Casula, M.; Rocca, D. *J. Chem. Phys.* **2007**, *127*, 014105.
(29) Spanu, L.; Sorella, S.; Galli, G. *Phys. Rev. Lett.* **2009**, *103*, 196401.
(30) Benali, A.; Shulenburger, L.; Romero, N. A.; Kim, J.; von Lilienfeld, O. A. *J. Chem. Theory Comput.* **2014**, *10*, 3417−3422.
(31) Ganesh, P.; Kim, J.; Park, C.; Yoon, M.; Reboredo, F. A.; Kent, P. R. C. *J. Chem. Theory Comput.* **2014**, *10*, 5318−5323.
(32) Dubecký, M.; Jurečka, P.; Derian, R.; Hobza, P.; Otyepka, M.; Mitas, L. *J. Chem. Theory Comput.* **2013**, *9*, 4287−4292.
(33) Dubecký, M.; Derian, R.; Jurečka, P.; Mitas, L.; Hobza, P.; Otyepka, M. *Phys. Chem. Chem. Phys.* **2014**, *16*, 20915−20923.
(34) Björkman, T.; Gulans, A.; Krasheninnikov, A. V.; Nieminen, R. M. *Phys. Rev. Lett.* **2012**, *108*, 235502.
(35) Perdew, J. P.; Schmidt, K. Jacob's ladder of density functional approximations for the exchange-correlation energy. AIP Conference Proceedings, Antwerp, Belgium, June 8−10, 2001; pp 1−20.
(36) Dion, M.; Rydberg, H.; Schröder, E.; Langreth, D. C.; Lundqvist, B. I. *Phys. Rev. Lett.* **2004**, *92*, 246401.
(37) The l_1-norm of $\Delta\rho$ is defined by $\int_{\text{cell}}|\Delta\rho(\mathbf{r})|d^3r/N$, where N is the number of atoms per unit cell. This quantity is used to characterize the charge redistribution of the system.
(38) Ferri, N.; DiStasio, R. A., Jr; Ambrosetti, A.; Car, R.; Tkatchenko, A. *Phys. Rev. Lett.* **2015**, *114*, 176802.
(39) Feynman, R. P. *Phys. Rev.* **1939**, *56*, 340−343.
(40) Cartz, L.; Srinivasa, S. R.; Riedner, R. J.; Jorgensen, J. D.; Worlton, T. G. *J. Chem. Phys.* **1979**, *71*, 1718−1721.
(41) Girifalco, L.; Lad, R. *J. Chem. Phys.* **1956**, *25*, 693−697.
(42) Olsen, T.; Yan, J.; Mortensen, J. J.; Thygesen, K. S. *Phys. Rev. Lett.* **2011**, *107*, 156401.
(43) Kim, J.; Esler, K. P.; McMinis, J.; Morales, M. A.; Clark, B. K.; Shulenburger, L.; Ceperley, D. M. *J. Phys.: Conf. Ser.* **2012**, *402*, 012008.
(44) Esler, K.; Kim, J.; Shulenburger, L.; Ceperley, D. *Comput. Sci. Eng.* **2012**, *14*, 40−51.
(45) Rasch, K. M.; Hu, S.; Mitas, L. *J. Chem. Phys.* **2014**, *140*, 041102.

DOI: 10.1021/acs.nanolett.5b03615
Nano Lett. 2015, 15, 8170−8175